DEPARTMENT OF THE INTERIOR

U.S. GEOLOGICAL SURVEY

In-Situ Stress Project,

Technical Report Number 3:

Analysis of Fractures from Borehole Televiewer Logs in a 500 m-Deep Hole at Xiaguan, Yunnan Province, Southwest China

by

Springer, J.E.[1], Zhai Qingshan[2], Zoback, M.D.[3], and Li Fangquan[2]

U.S. Geological Survey

Open-File Report 87-432

Prepared in cooperation with the State Seismological Bureau of China, the University of Wisconsin, and Stanford University.

1 Menlo Park, CA

2 Inst. of Crustal Dynamics Beijing, China

3 Stanford Univ., Stanford, CA

1987

CONTENTS

FIGURES

UNITED STATES
DEPARTMENT OF THE INTERIOR
GEOLOGICAL SURVEY

ANALYSIS OF FRACTURES FROM BOREHOLE TELEVIEWER LOGS IN A 500 M-DEEP HOLE AT XIAGUAN, YUNNAN PROVINCE, SOUTHWEST CHINA

J.E. Springer, Zhai Qingshan, M.D. Zoback, and Li Fangquan

ABSTRACT

Fractures from a 500 m-deep hole in the Red River fault zone were analyzed using an ultrasonic borehole televiewer. Four hundred eighty individual fractures were identified between 19 m and 465 m depth. Fracture frequency had no apparent relation to the major stratigraphic units and did not change systematically with depth. Fracture orientation, however, did change with stratigraphic position.

The borehole intersected 14 m of Cenozoic deposits, 363 m of lower Ordovician clastic sediments, and 106 m of older ultramafic intrusions. The clastic sequence was encountered again at a depth of 484 m, suggesting a large fault displacement. Fractures in the top 162 m of the sedimentary section appear randomly distributed. Below that depth, they are steeply dipping with northerly and northwesterly strikes, parallel to the major active faults in the region. Fractures in the ultramafic section strike roughly east-west and are steeply dipping. These orientations are confined to the ultramafic section and are parallel to an older, inactive regional fault set.

INTRODUCTION

As part of a joint Sino - U.S. venture, hydraulic fracturing stress measurments were performed in a 500 m - deep hole at Xiaguan, southwest China in October, 1983. The experiments were carried out in the China Earthquake Prediction Test Site, which is a 60,000 square kilometer area located in Yunnan Province, southwest China (Fig. 1). The well site is located on the eastern bank of Erhai Lake, which is part of the Dianxi basin, a probable pull-apart associated with the Red River fault zone (Fig. 2). Before the stress measurements were performed, a borehole televiewer (BHTV) log was run in order to inspect the condition of the well, select intervals for hydraulic fracturing and evaluate pre-existing fractures. This was the first time that the BHTV was used for earthquake research in China.

Natural fractures are one of the most important and least understood phenomena in rock mechanics. They exert a profound influence on ground water flow, heat flow, seismic velocity,

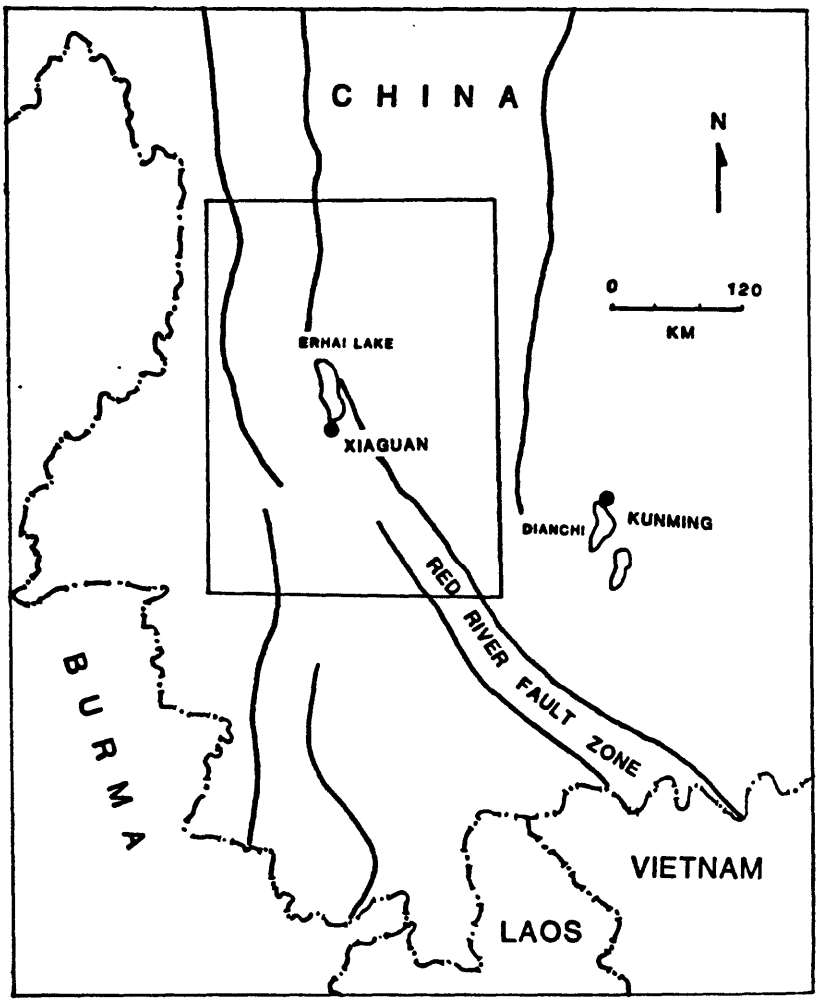

Figure 1. Location map showing the Earthquake Prediction Test Site in southwest China. The rectangle indicates the location of fig. 2.

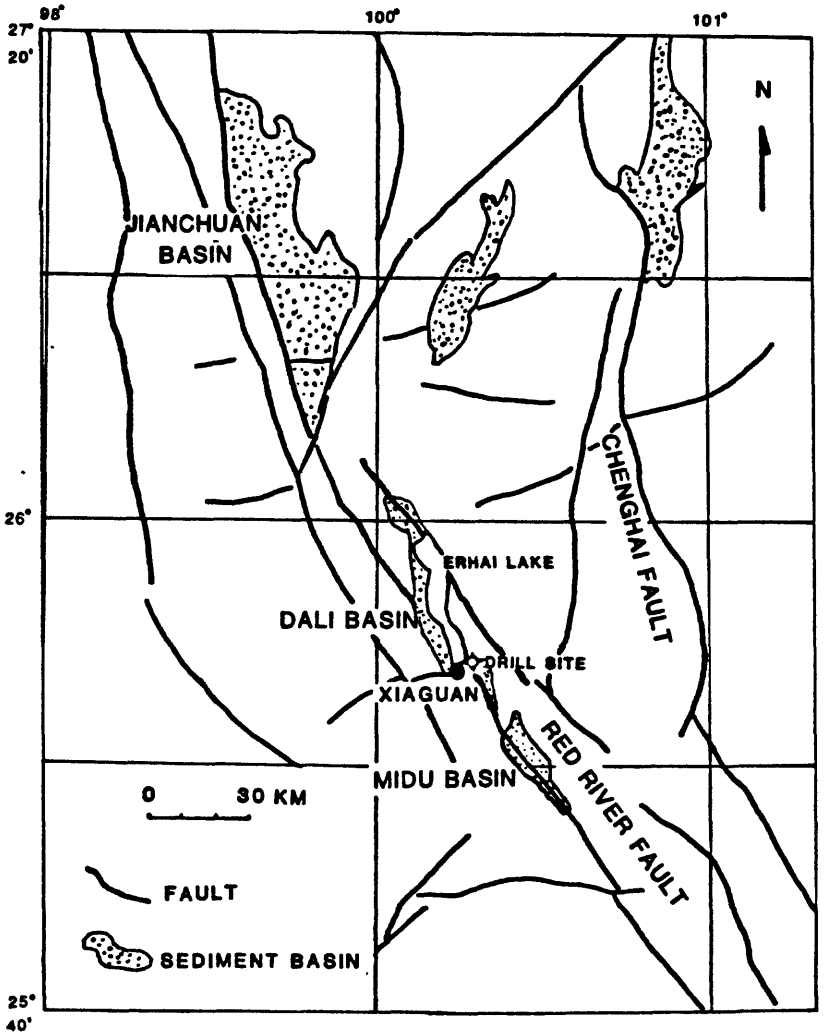

Figure 2. Map showing the main tectonic features of the Earthquake Prediction Test Site.

anisotropy, and effective elastic moduli. Their genesis is related to the stresses that existed when they were formed and their presence affects the way the earth's crust responds to contemporary tectonic stresses. Very few studies of fractures at depth have been undertaken, particularly in the seismically active area of southwest China. In this paper, we present the results of in-situ fracture studies in the test borehole.

The Xiaguan well was continuously logged with the BHTV. The orientation and distribution of fractures were determined from the log. These data were evaluated to determine the variations in fracture distribution with depth and what relation, if any, could be found between the observed fractures and what is known about the regional stress field and geologic history.

GEOLOGIC BACKGROUND OF THE TEST SITE

The Earthquake Prediction Test Site lies in a mountainous area along the east flank of the eastern syntaxial bend of the Himalayan mountain chain. The high elevation of the region is a result of the collision between the Indian and Eurasian plates during the last 30 m.y. The most prominent active tectonic feature is the Red River fault which trends northwest from the Gulf of Tonkin to at least as far as Xiaguan and has a total length of at least 900 km (Allen et al., 1984). The dominant sense of slip is right lateral although some segments have a large normal component. While there have not been any major historic earthquakes along the fault, geologic evidence indicates repeated Holocene movements (Allen, et al., 1984). North of Xiaguan, a series of more northerly trending faults appear to be a continuation of the Red River fault zone.

The Red River fault consists of a northeast branch and a southwest branch. The northeast branch is characterized by right-lateral strike-slip, based on the relation of the fault to strata on both sides, on the sense of drag of bedding along the fault, and a cleavage belt parallel to the fault plane (Han Yuan et al., 1983). Mountain ridges and stream systems that it crosses are offset dextrally. Horizontal slip rate estimates vary from 2 to 5 mm per year (Allen et al., 1984) to about 8 mm per year (Chang Jing, et al., 1983).

The southwest branch has a considerable amount of vertical throw. Evidence for this is from triangular facets on ridges (Allen, et al., 1984) and geophysical logs from the Dali basin which indicate a Quaternary depositional thickness of about 2200 m. During the past 2 m.y., the average vertical slip rate on the fault has been around 1.1 mm per year (Chang Jing, et al., 1983). North of Xiaguan, the Red River fault zone becomes less well-defined. Its main trace has a more northerly trend and follows the Jinsha River Valley.

There are several faults parallel to the Red River fault zone. Most, but not all of them lie to the southwest of the Red River fault. Northeast of the Red River fault, most active faults

have dip-slip displacement and some have a sinistral component (Allen, et al., 1984; Kan, et al., 1977). There are also east-west-trending faults in the area. The largest one is the Xierhe fault which controls the southern margin of the Ehrhai basin.

The borehole is located in a structurally complex area at the intersection of the Red River fault zone, the Chenghai fault zone, and an older east-west-trending tectonic zone near Xiaguan. Although the portion of the Red River fault immediately south of Xiaguan has not had a significant earthquake in the last 300 years, the seismic activity to the north is rather high. In March, 1925, a magnitude M=7 earthquake occurred in Dali County. Some shocks with magnitudes of 5 to 6 have occurred and the latest two took place in succession in May, 1978 near the drill site.

A lithologic summary of the hole is shown in fig. 3. The upper 380 m of the well encountered a lower Ordovician clastic sequence of fine-grained sandstone, shales, and quartz-rich sandstone. Ultramafic intrusive rocks were encountered at 380 m. The clastic sequence was again encountered at 484 m, suggesting the presence of either a thrust fault or a large amount of lateral displacement on a strike-slip fault.

FRACTURE STUDIES

The BHTV was used to examine the distribution of natural fractures. The BHTV system consists of a downhole logging tool and surface instruments. Zemanek et al (1969) describe the tool in detail. The tool consists of a centralized logging sonde with a rotating acoustic piezoelectric transducer. The transducer emits 1 MHz pulses focused in a 3 degree beam at a rate of about 1800 pulses per second. It rotates at three revolutions per second as the tool is logged up the hole at a speed of 1.5 m per minute. A flux-gate magnetometer provides orientation with respect to magnetic north. The surface instruments consist of a winch, surface panel, video cassette recorder, two oscilloscopes and a camera.

The acoustic pulses from the transducer are transmitted to the borehole wall and reflected back to the transducer which then acts as a reciever. The signal is sent through the logging cable to the surface for recording and processing. The amplitude of the reflected pulse is output as a function of brightness on a three-axis oscilloscope. Each sweep on the scope is triggered to magnetic north. The oscilloscope display is photographed as successive sweeps move up the scope to make a record of the data. The resulting log is a sonic "picture" of the inside of the hole as if it were split down the middle and laid flat (fig. 4a). The raw data are also recorded on video tape.

Resolution of the televiewer depends on hole diameter, wall roughness, and the acoustic impedence contrast between the bore hole fluid and the wall rock. Hard rock generally reflects more signal than soft rock. Clear water produces a much better

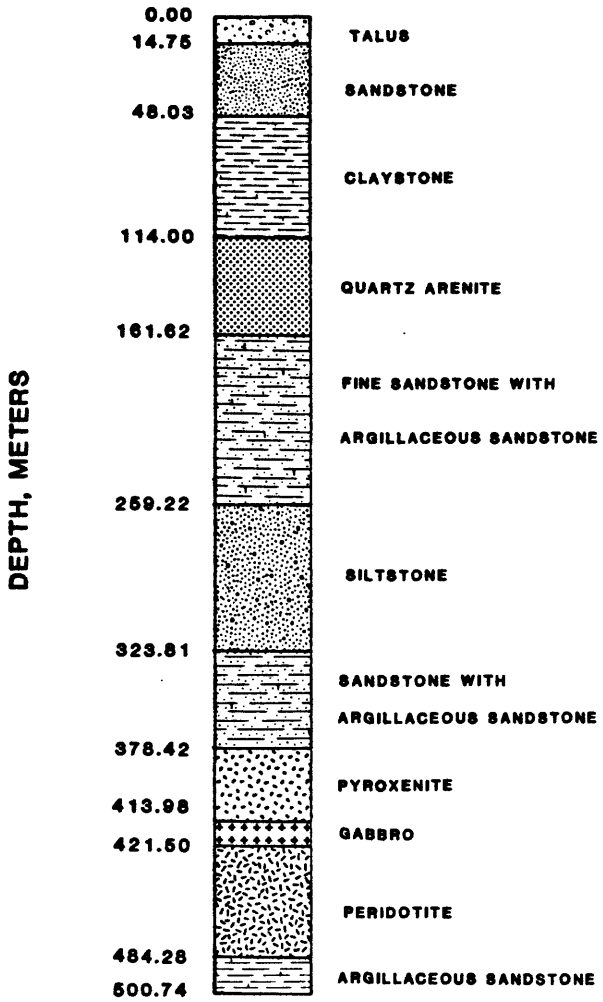

Figure 3. Lithologic summary of the Xiaguan borehole.

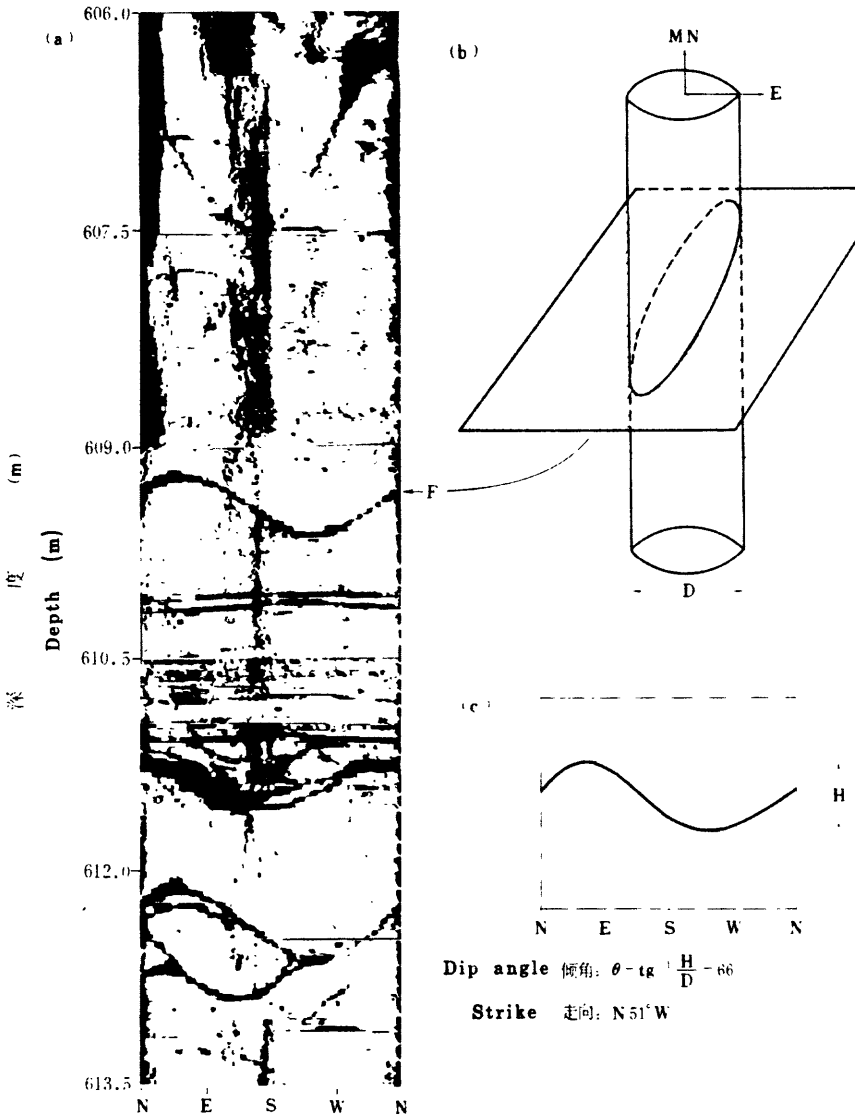

Figure 4. Example of a typical televiewer log showing inclined fractures crossing the borehole.

reflected signal than heavy mud. A rough wall contains many small oblique surfaces and reflects much of the energy away from the transducer so that it makes detection of fine features difficult (Seeburger and Zoback, 1982). Essentially, the televiewer log presents the smoothness of the borehole wall. Where the smoothness is perturbed by a fracture, a dark pattern appears on the log. If it is a vertical fracture intersecting the well bore axis, the fracture appears as two dark vertical lines 180 degrees apart. If there is an inclined fracture or bedding plane intersecting the well bore, it shows up as a sinusoidal curve on the log (fig. 4). Because the oscilloscope is triggered on magnetic north, the orientation of the sinusoid can be easily determined on the televiewe picture. The strike of the fracture is the direction that is 90 degrees from the peak and 90 degrees from the trough on the sinusoid. The dip angle of the fracture is calculated from the amplitude h of the sinusoid by:

$$\text{dip} = \tan^{-1} h/d$$

where d is the hole diameter. As an example, fig 4 (a) is a BHTV log of a 7.5 m section of hole. The dip direction of the fracture illustrated in fig. 4 (b) and (c) is to the S39W. The dip angle is 66 degrees, and the strike is N51W. The horizontal and vertical scales are different on the log. For a hole the size of the Xiaguan well, there is an approximate 4:1 horizontal exaggeration.

The BHTV was run continuously from 464.9 m to 19 m (at the bottom of the casing). The complete log is shown in the Appendix. Knowing the hole diameter from a caliper log, the orientations of the fractures were computed. Because they make a low angle with the hole, very steep dips are under-represented in the data. Only fractures (that cut completely across the borehole) were used in the analysis. Subhorizontal fractures were excluded because we judged them to be bedding and because the horizontal exaggeration makes accurate determination of low angle dips nearly impossible. We have identified a total of 480 natural fractures from the BHTV log.

A series of lower hemisphere equal-area plots of poles to fractures is shown in fig. 5. The entire logged section is presented in fig. 5 (a). There is a great deal of scatter in the data, however high-angle fractures with west and southwest dips are the most common. Fracture orientations at various depth intervals have stronger preferred orientations (fig. 5 b, c, d, and e). Comparing fig. 5 to the lithologic summary in fig. 3, it can be seen that the fracture orientations change with stratigraphic position. The uppermost section from 19 m to 113 m contains highly fractured sandstone and claystone. Immediately below it is a 49 m section dominated by quartz arenite. Fracture poles for these two sections are shown in fig. 5 (b). The dip pattern in this interval shows no obvious trends. At 162 m, where the lithology changes to a fine, argillaceous sandstone, a preferred orientation emerges. Most of the dips are between 50 and 75 degrees to the west and southwest (fig. 5 c). This

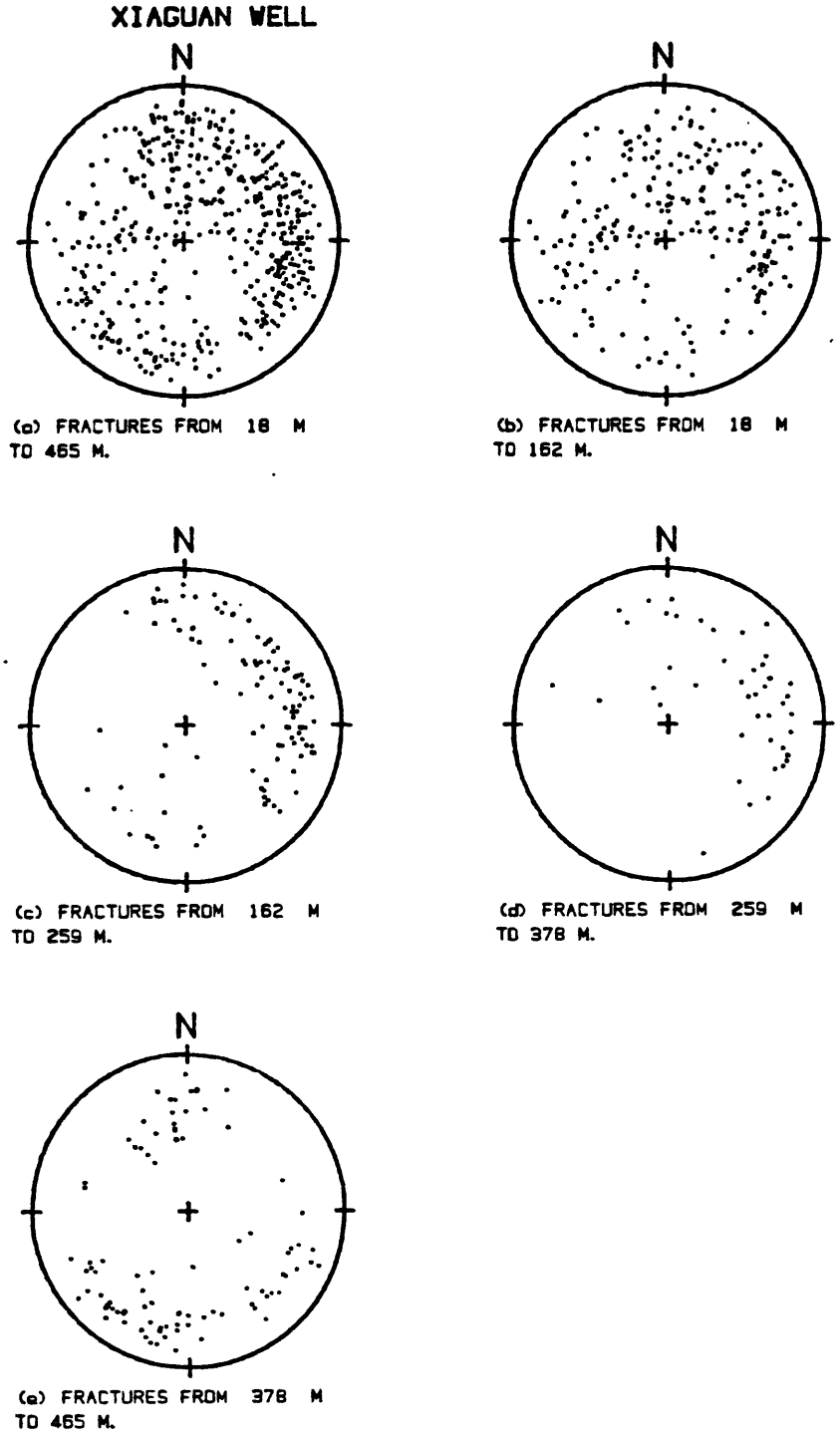

Figure 5. Lower hemisphere schmidt projections of poles to the fractures seen on the BHTV log. All the fractures are shown in (a). Fractures from the indicated depth intervals are shown in (b), (c), (d), and (e).

distribution persists through another lithologic change at 261 m and continues to the top of the ultramafic section (fig. 5 d).

The fracture orientation distribution changes in the ultramafic section (fig. 5 e). Here, most of the fractures dip steeply to the north and south. This probably represents a single near vertical set that strikes roughly west-northwest to east-west. Fractures in the clastic section below 484 m could not be sampled because the hole caved in on this section.

A more detailed representation of fracture orientations with depth is shown in fig. 6. In this figure, the data are plotted in a format similar to dip logs used in the petroleum industry. The vertical axis is depth and the horizontal axis is dip. The direction of dip is indicated by the arrow on the plotting symbol, with north toward the top of the page. Typical oil industry logs use a logarithmic scale on the dip angle axis because the configuration of their logging systems results in a decrease in accuracy as the dip angle approaches vertical. We use a linear scale on the dip angle axis because, with the televiewer data, the steep dips are actually more accurate than the shallow dips.

Between 150 m and 350 m, most of the dips are to the west and south and are moderately high angle. Most of the scatter in this interval occurs in short intervals around 165 m, 210 m, and 265 m. In several intervals of fig. 6, the dips are sparse and scattered. Some of these in the lower part of the well are intensely fractured zones and/or large washouts that are too dark and complex on the log to resolve individual fractures. The largest of these intervals is between 360 m and 396 m.

The formation where the borehole is located is intensely fractured. The entire hole was cored, but few intact cores were found and the longest one was less than 70 cm. A histogram of fracture frequency as a function of depth is shown in fig. 7. The class interval of the plot is 3 m. Fracture frequency does not show any systematic change with depth. Except for the fracture zone from 360 m to 396 m, the frequency of fractures visible on the BHTV log attains a maximum of 3 througoing fractures per meter. Between 360 an 396 m, where the hole was enlarged up to 35 cm, few distinct features could be seen. The fracture frequency in this interval is clearly much greater than 3 fractures per meter.

DISCUSSION

Fracture orientations in the top 160 m of the well appear to be randomly distributed. Below that depth, the fractures appear to reflect the main tectonic features of the region. High-angle fractures from 162 m to 378 m with southwest dips are parallel to the Red River fault zone and those with more westerly dips are parallel to the north- to northeast-trending fault set in the region (fig. 2). In the ultramafic section below 378 m, the fracture strikes are roughly parallel to the east-west trending

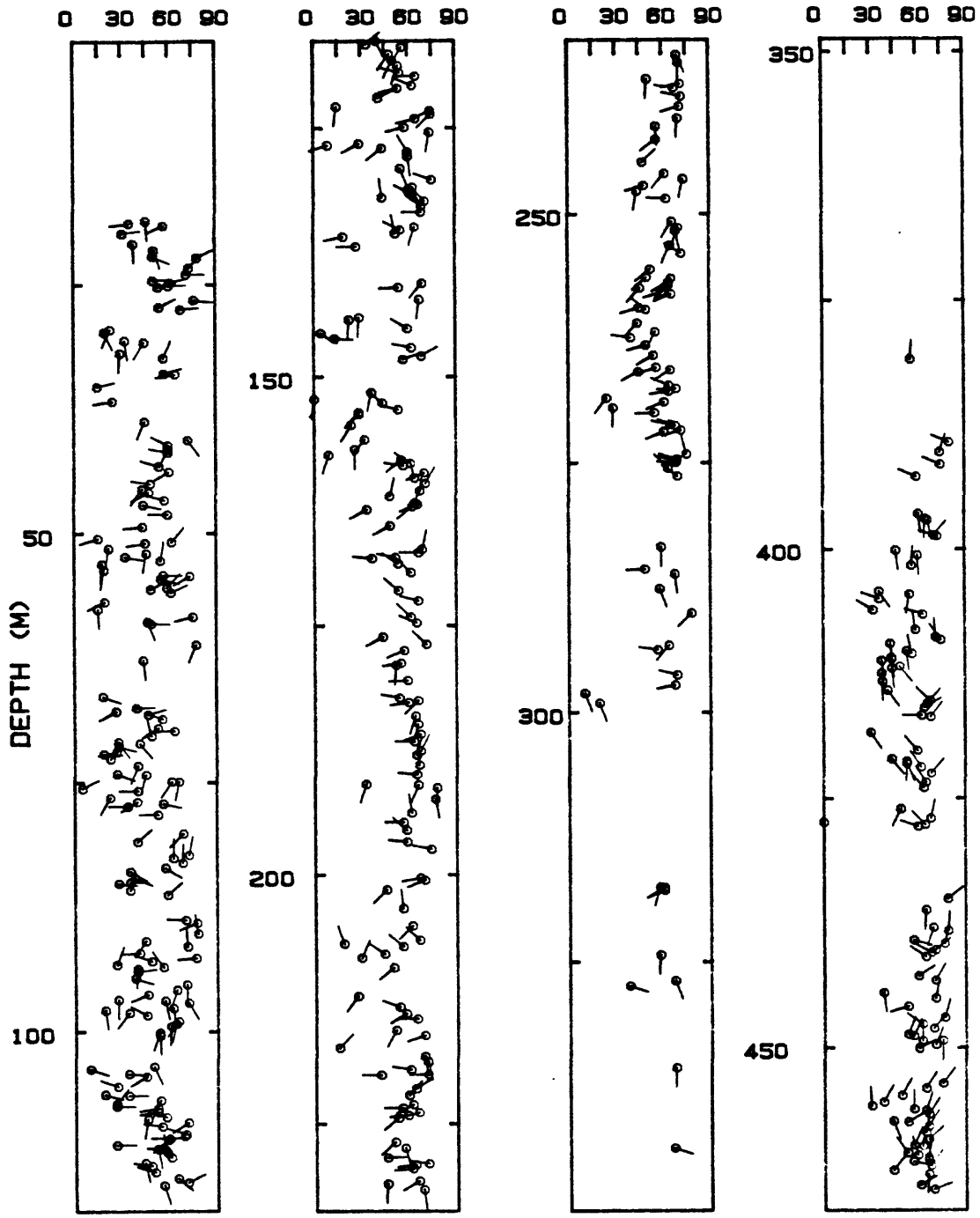

Figure 6. Dip log presentation of fractures seen in the Xiaguan well. The horizontal axis is dip angle. The arrow on the plotting symbol represents the dip direction with north being to the top of the page.

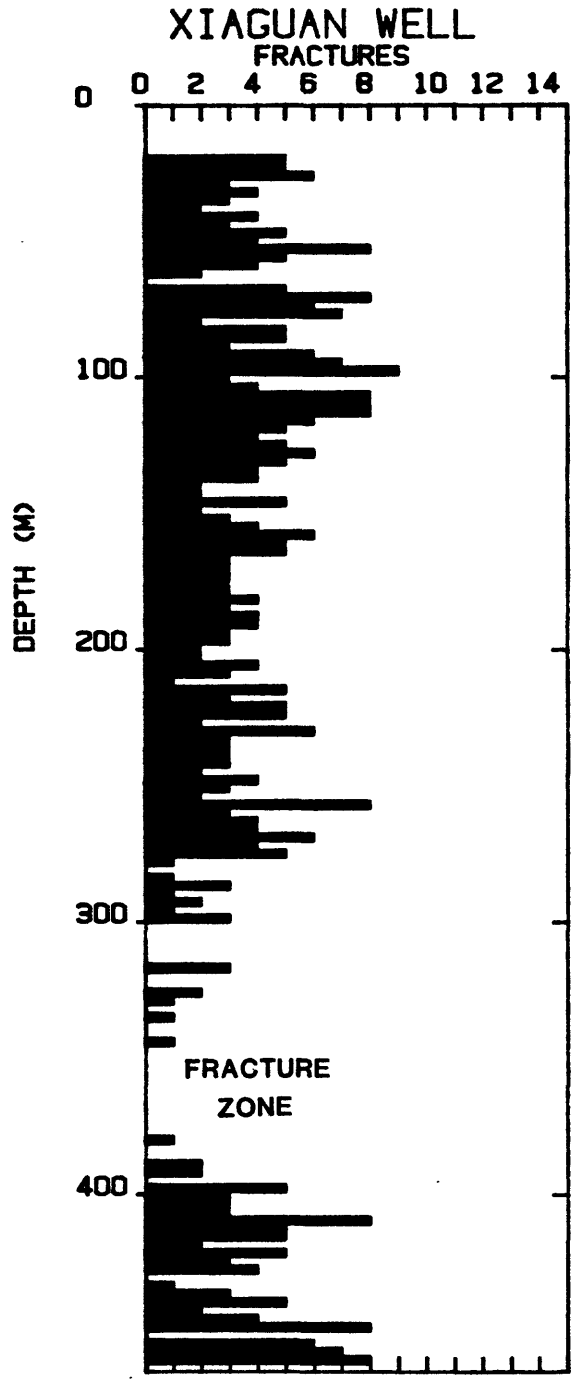

Figure 7. Plot of fracture frequency vs depth.

tectonic zone in the region. The tectonics of the region suggest that fractures between 162 m and 378 m are related to active faulting while most of the fractures in the ultramafic section may be related to the older structural fabric of the region.

The orientation of stresses is generally consistent with movement along westerly and southwesterly dipping faults. Kan et al. (1977) compiled focal mechanisms from earthquakes in southwest China. Although the P- and T-axes of the focal mechanisms are not a reliable indicator of stress directions (McKenzie, 1969), a compilation of them can reveal a general trend. A variety of different types of mechanisms were calculated, but the vast majority of them are either strike-slip or normal. There is a large amount of scatter in the directions of the P- and T- axes, but the pattern is consistent with generally north-south compression and east-west extension. Movement on northwest-trending faults is usually dextral and movement on north- and northeast-trending faults is usually normal and/or sinistral.

Hydraulic fracturing stress measurements in the Xiaguan hole indicate a north-northeast maximum horizontal stress orientation (Li et al., 1986). Further evidence of the stress field comes from overcoring measurements performed by the Seismological Bureau of Yunnan Province. These measurements show a great deal of scatter in the orientations, due, in part to the effects of topography. The general trend, however agrees with the focal mechanisms.

As a first approximation, the east-west-striking, high-angle fractures in the ultramafic section appear roughly normal to the major principal stress in the region. This orientation does not appear consistent with movement on them. Because of its orientation and because the fracture set does not extend into the clastic section above it, we conclude that it originated from a past stress event.

ACKNOWLEDGEMENTS

Jack Healy provided support and encouragement for the project. Bezalel Haimson was helpful in coordinating and supervising the field operations. Joe Svitek ran the televiewer log in the field. Zhao Guozhu provided valuable geologic information. Doug Myren reviewed the paper and made helpful comments.

REFERENCES

Allen, C.R., Gillespie, A.R., Han Yuan, Sieh, K.E., Zhang Buchan, and Zhu Chengnan, 1984, Red River and associated faults, Yunnan Province, China; Quaternary geology, slip rates, and seismic hazard: Geological Society of America Bulletin, v.95, no.6, pp.686-700.

Chang Jing, et al., 1983, Seismogeological report on Dinxi Test Site in 1982 (in Chinese): Proceedings of Seismo-geology

Reports, Geological Team, Seismological Bureau of Yunnan Province, v.2, pp.89-122.

Han Yuan, et al., 1983, Geological feature studies on Red River fault in Yunnan Province (in Chinese): Proceedings of Seismogeology Reports, Geological Team, Seismological Bureau of Yunnan Province, v.2, pp.5-87.

McKenzie, D.P., 1969, The relationship between fault plane solutions for earthquakes and the directions of the principal stresses: Seismological Society of America Bulletin, v. 5, pp.591-601.

Seeburger, D.A, and Zoback, M.D., 1982, The distribution of natural fractures and joints at depth in crystalline rock: Journal of Geophysical Research, v.87, no.B7, pp.5517-5534.

Zemanek, J., Caldwell, R.L., Glenn, E.E., Jr., Holcomb, S.V., Norton, L.F., and Strauss, A.D.J., 1969, The borehole televiewer - a new logging concept for fracture location and other types of borehole inspection: Journal of Petroleum Technology, v.264, pp.762-774.

APPENDIX

Borehole Televiewer Log of the Xiaguan Hole

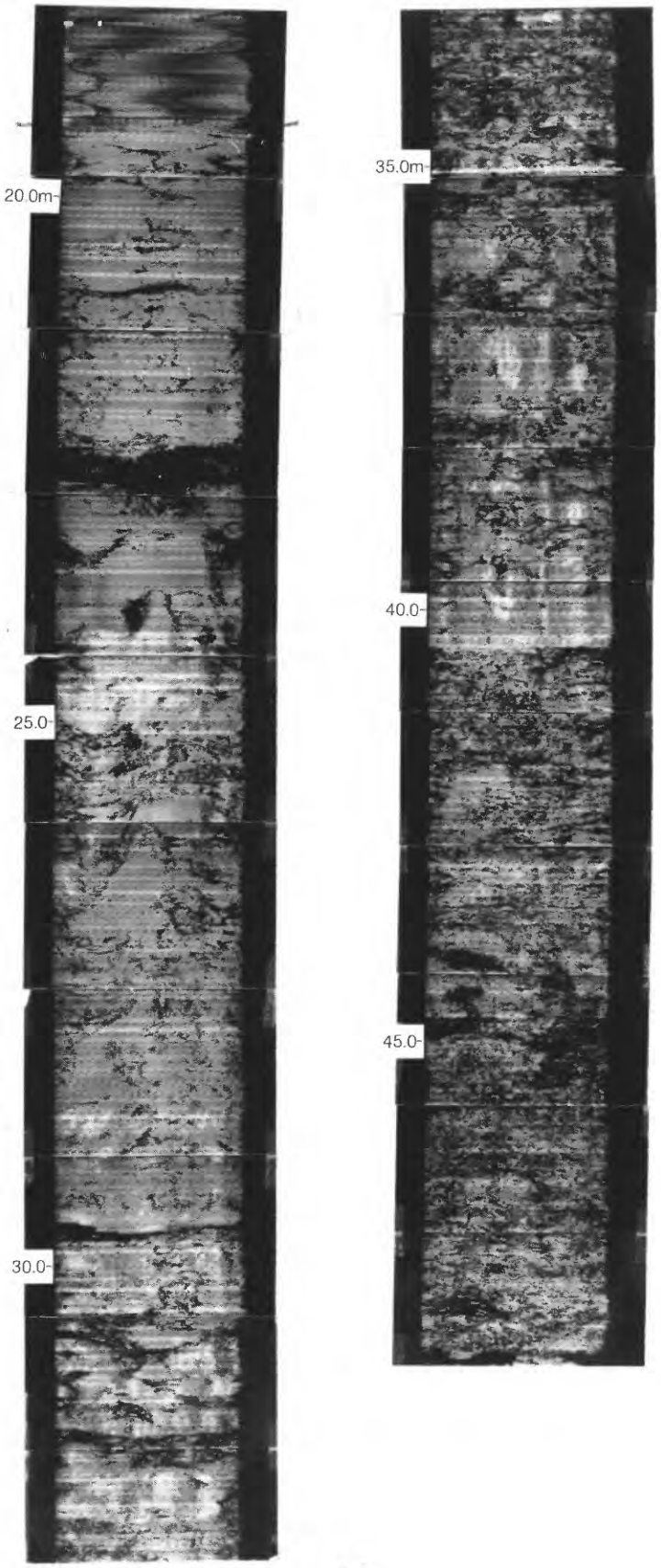
20.0m
25.0
30.0
35.0m
40.0
45.0

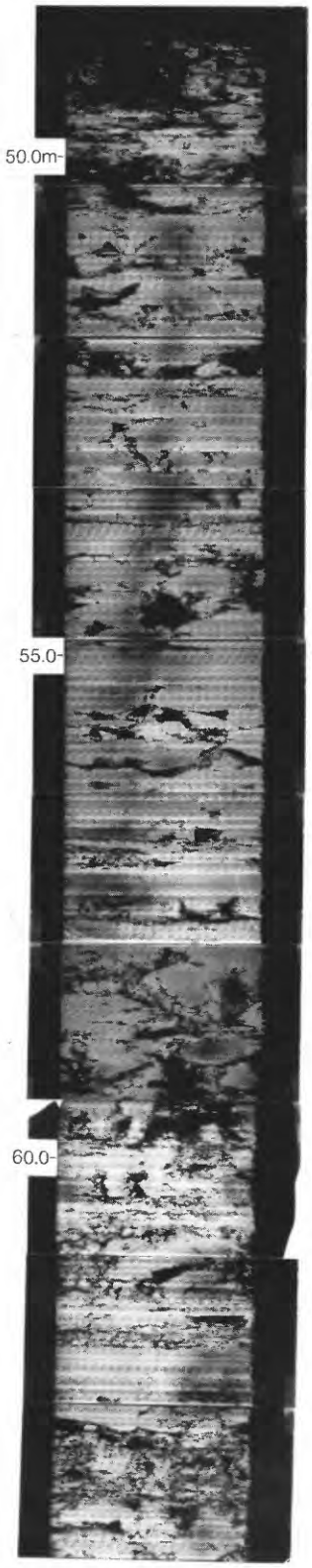

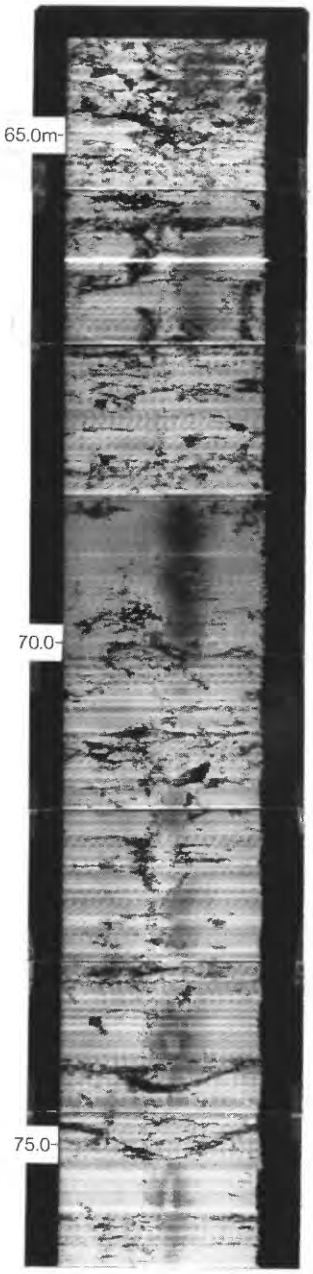

No picture

from 77.7m to 83.8m.

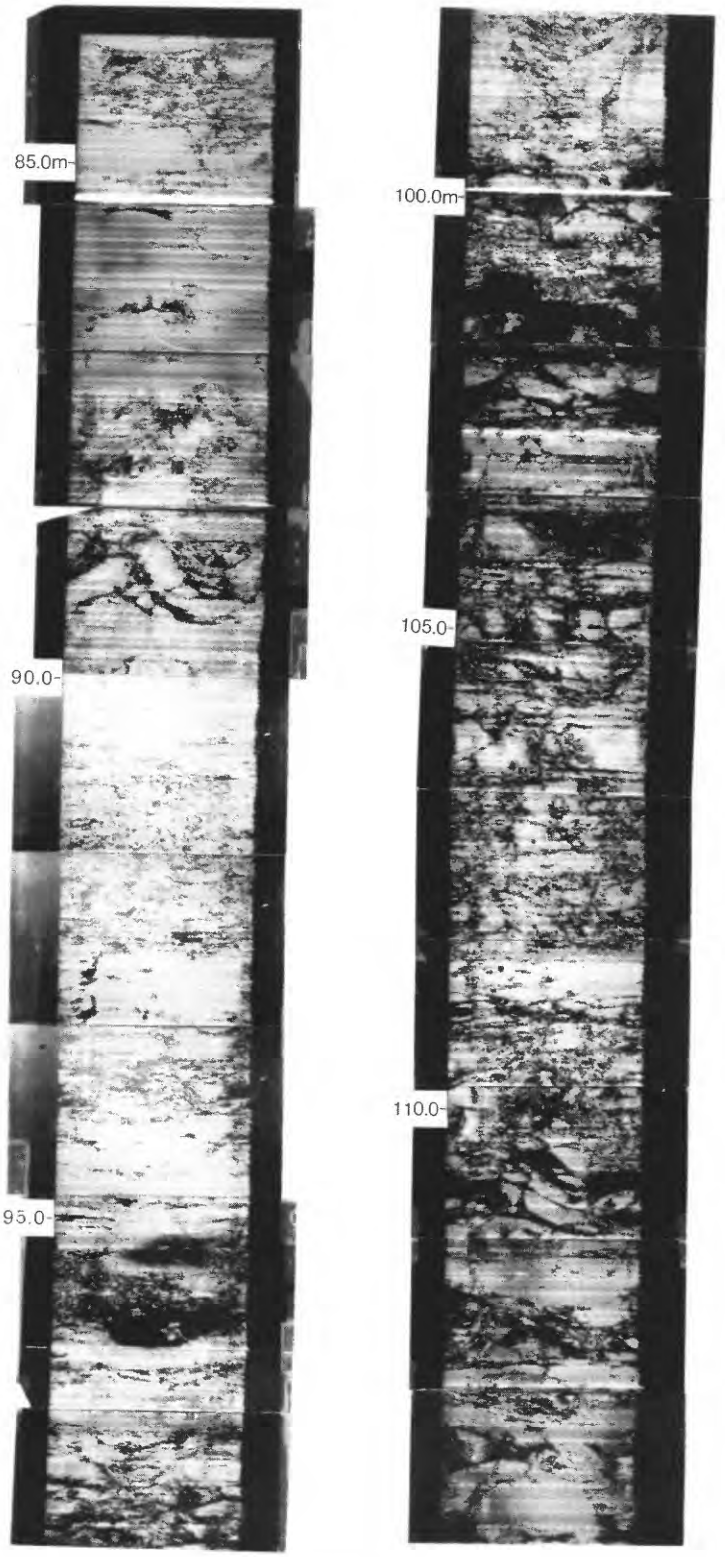
85.0m
90.0
95.0
100.0m
105.0
110.0

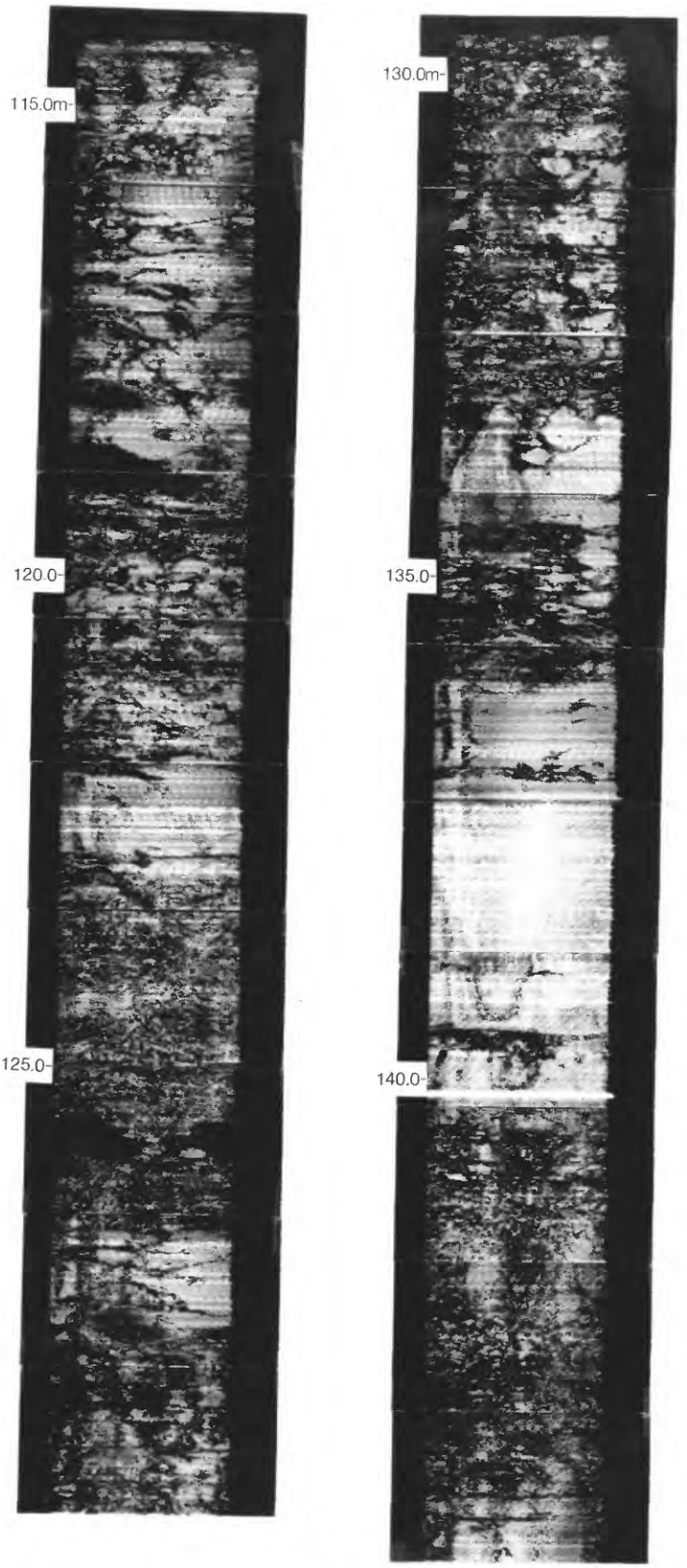
115.0m
120.0
125.0
130.0m
135.0
140.0

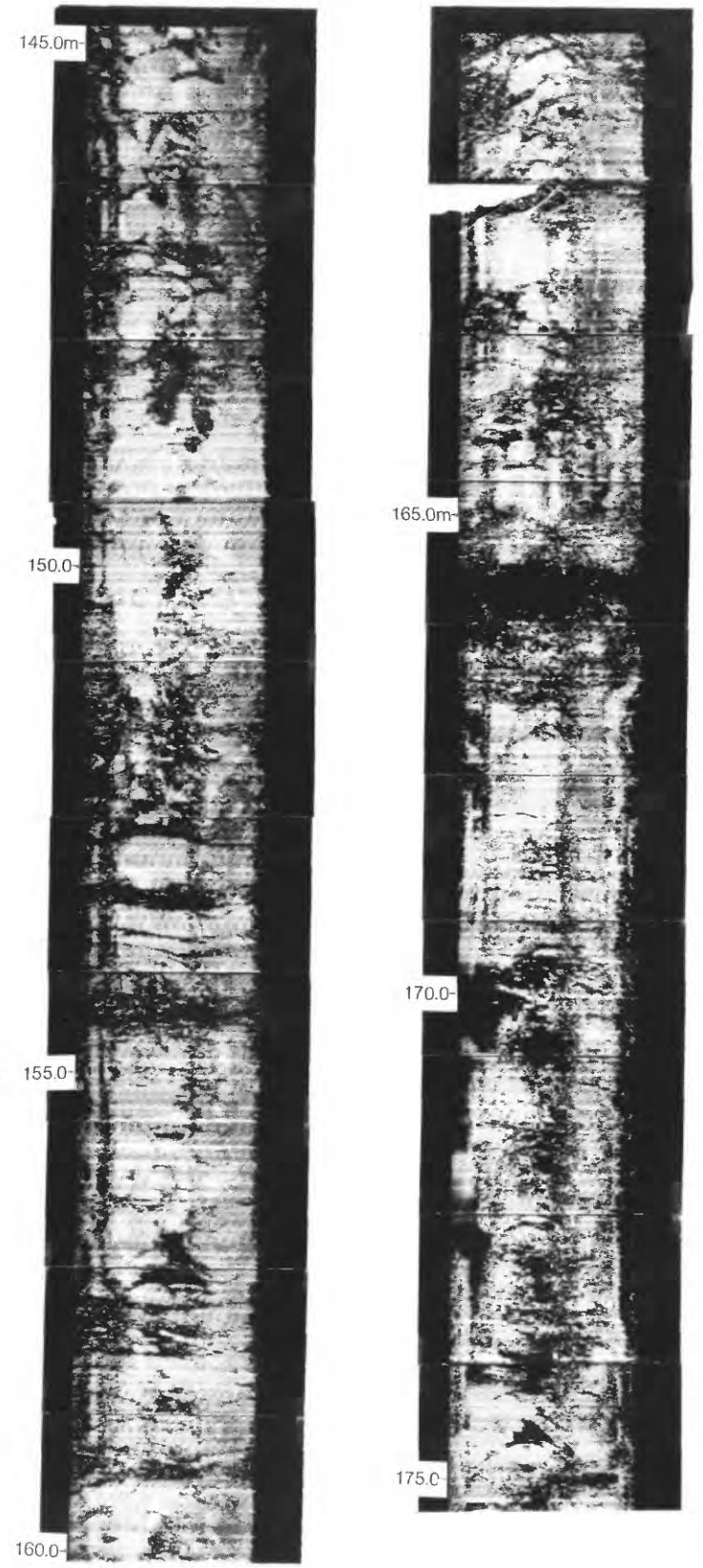
145.0m
150.0
155.0
160.0
165.0m
170.0
175.0

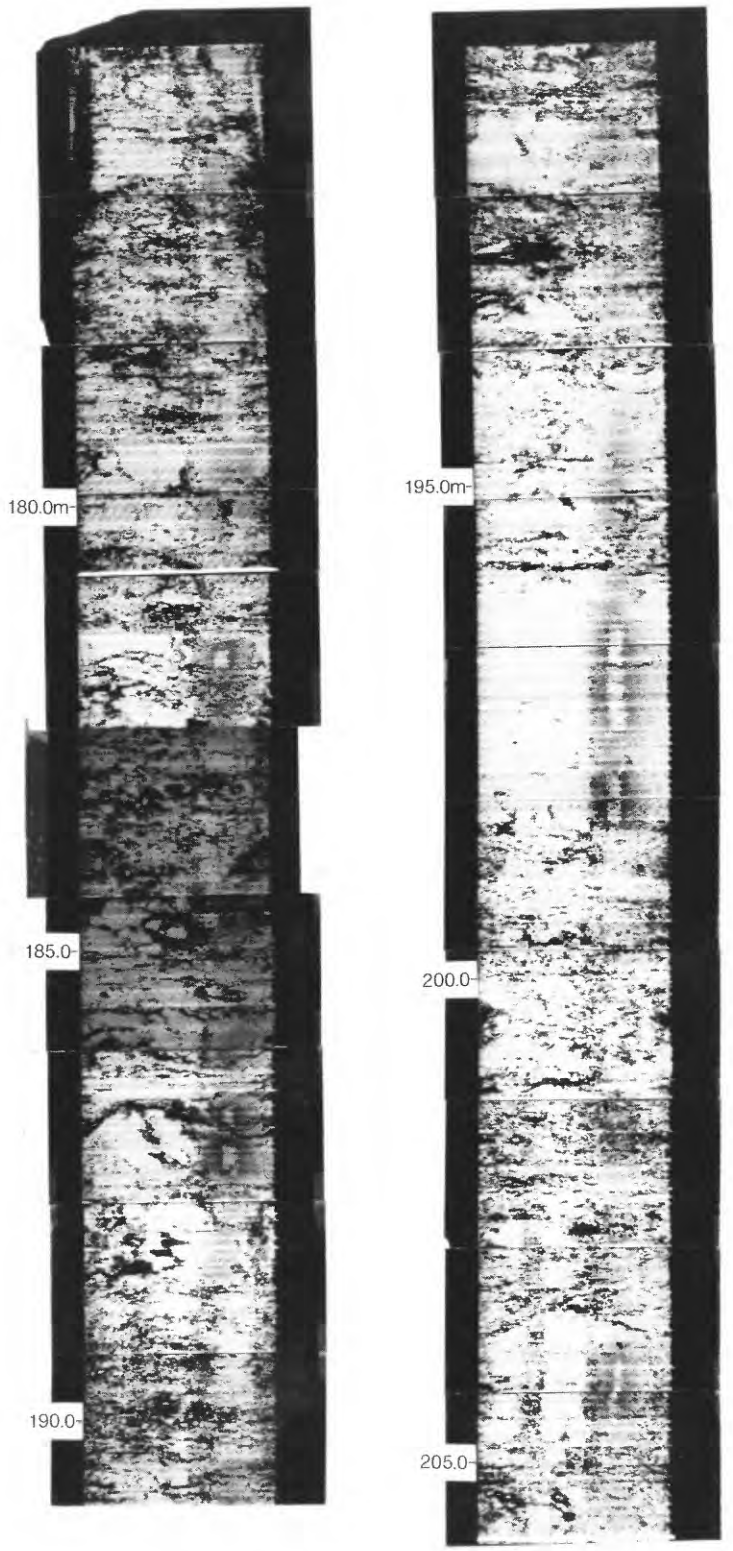
180.0m
185.0
190.0
195.0m
200.0
205.0

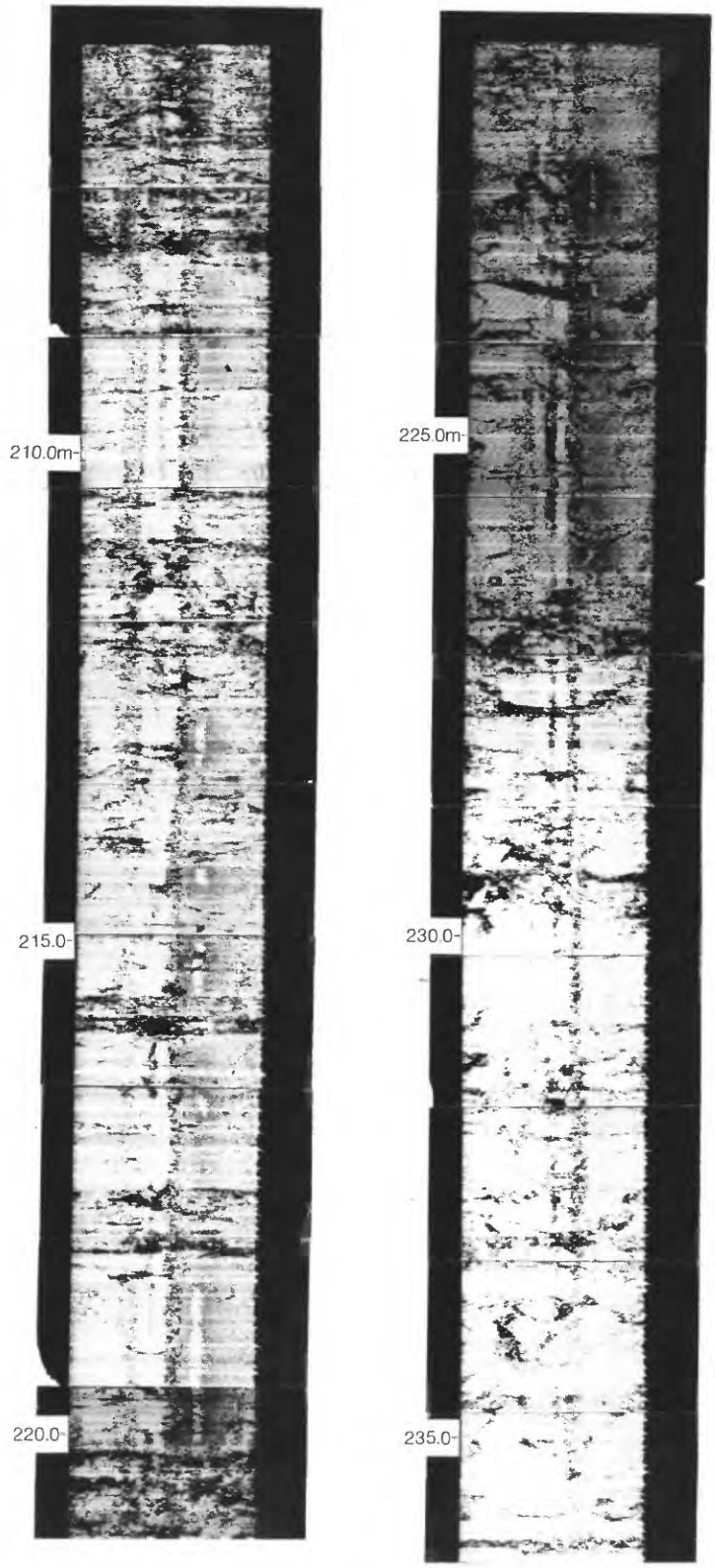
210.0m
215.0
220.0
225.0m
230.0
235.0

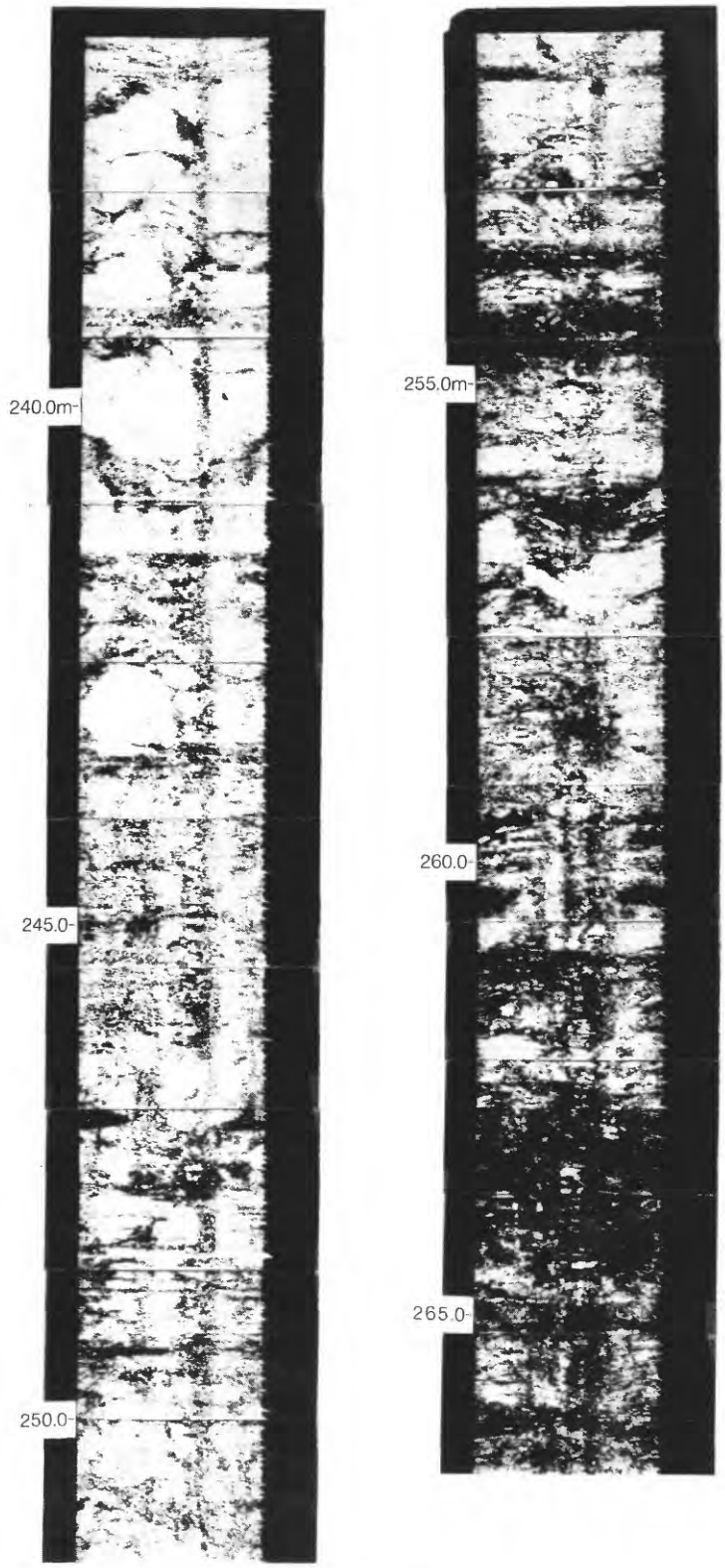
240.0m
245.0
250.0
255.0m
260.0
265.0

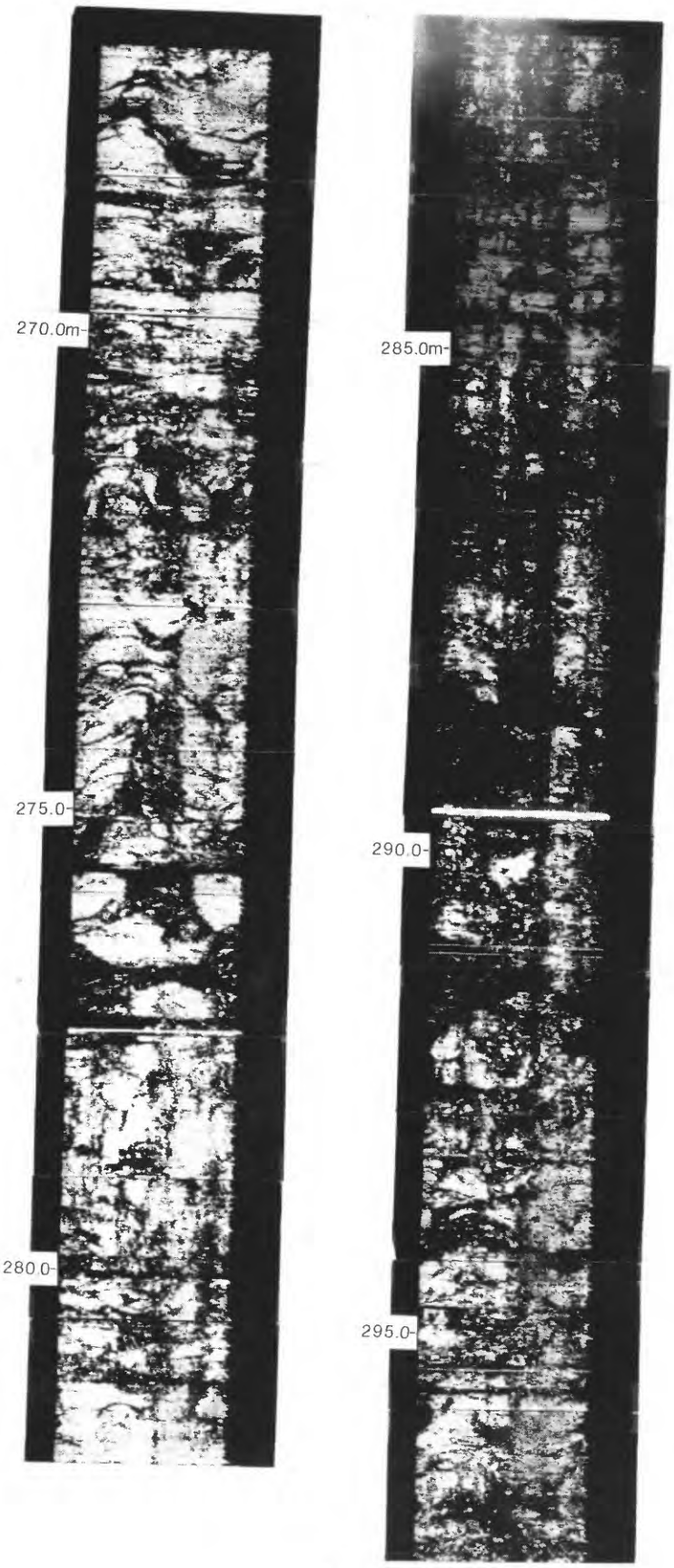
270.0m-
275.0-
280.0-
285.0m-
290.0-
295.0-

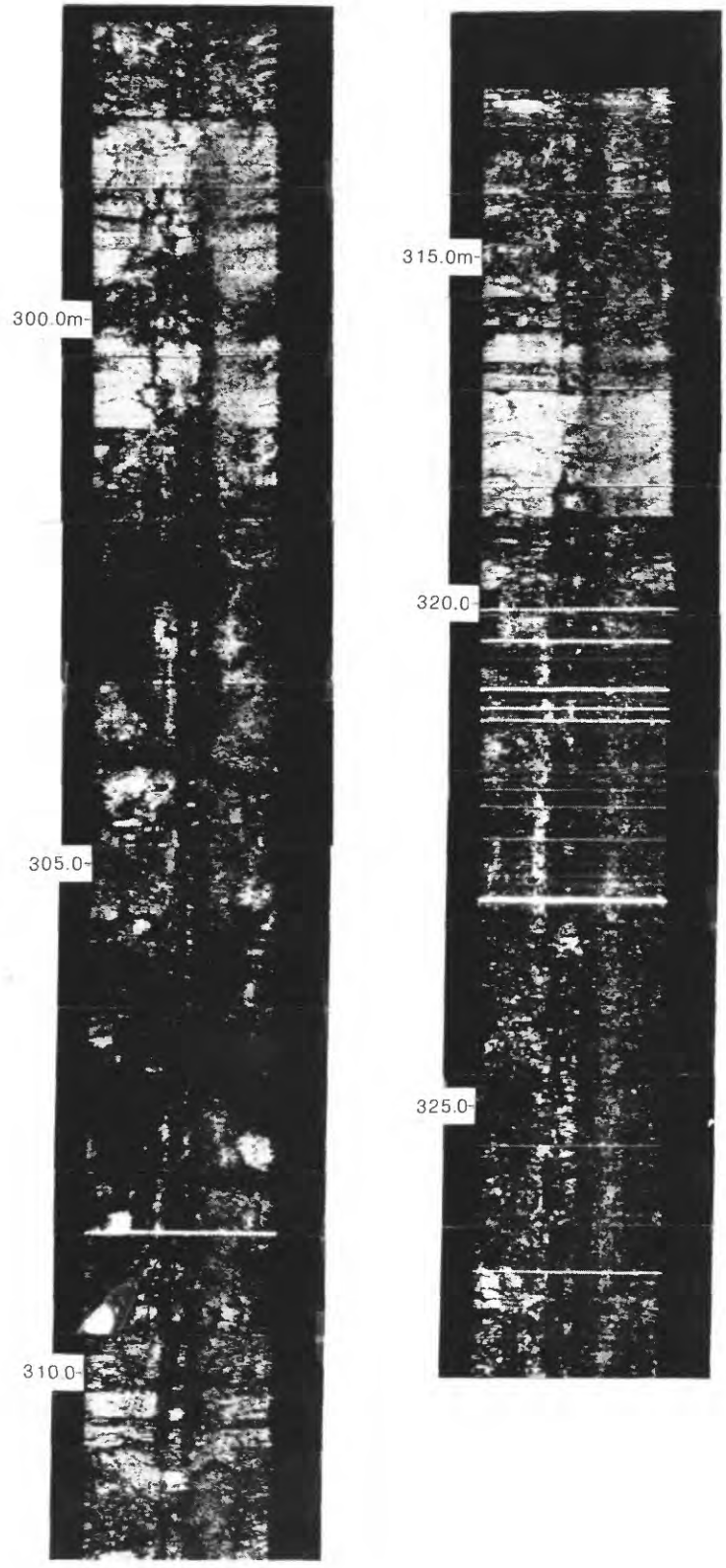
300.0m
305.0
310.0
315.0m
320.0
325.0

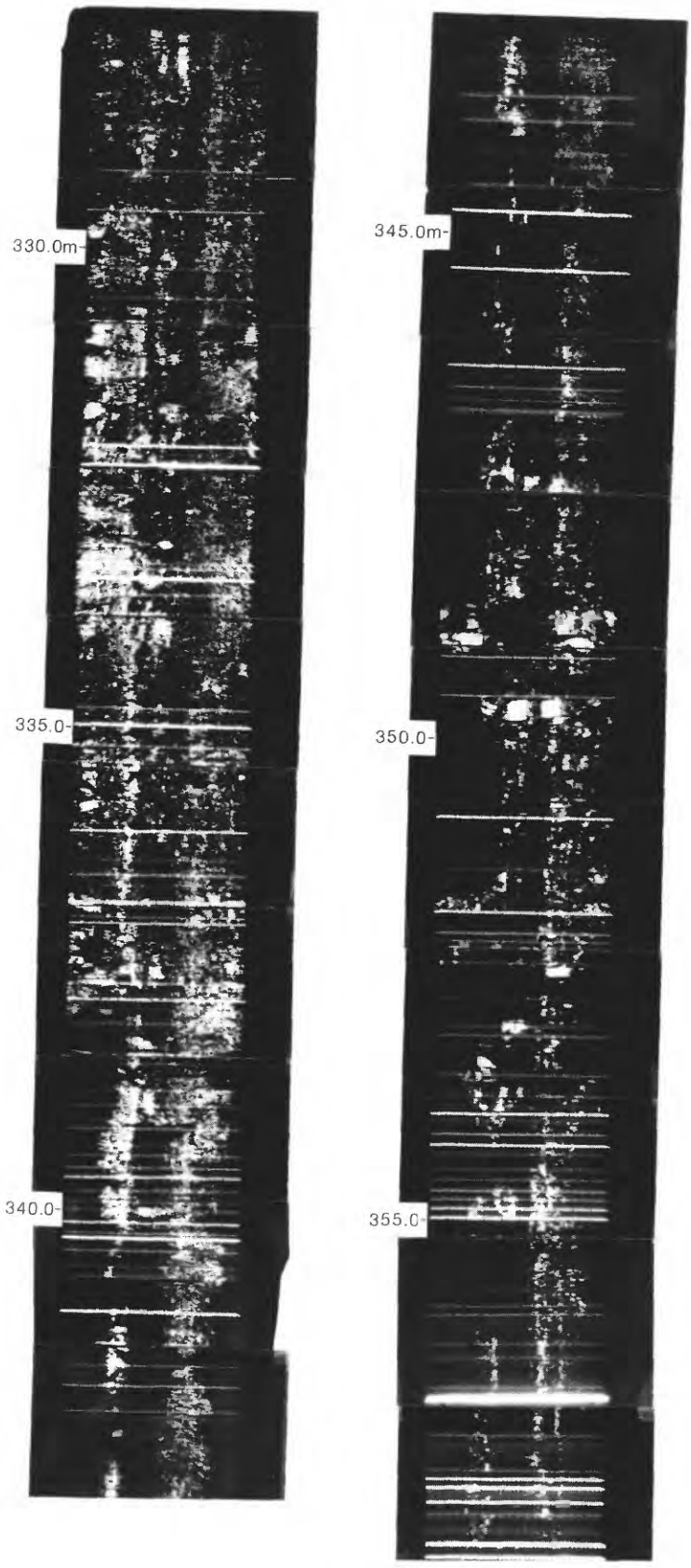
330.0m
335.0
340.0
345.0m
350.0
355.0

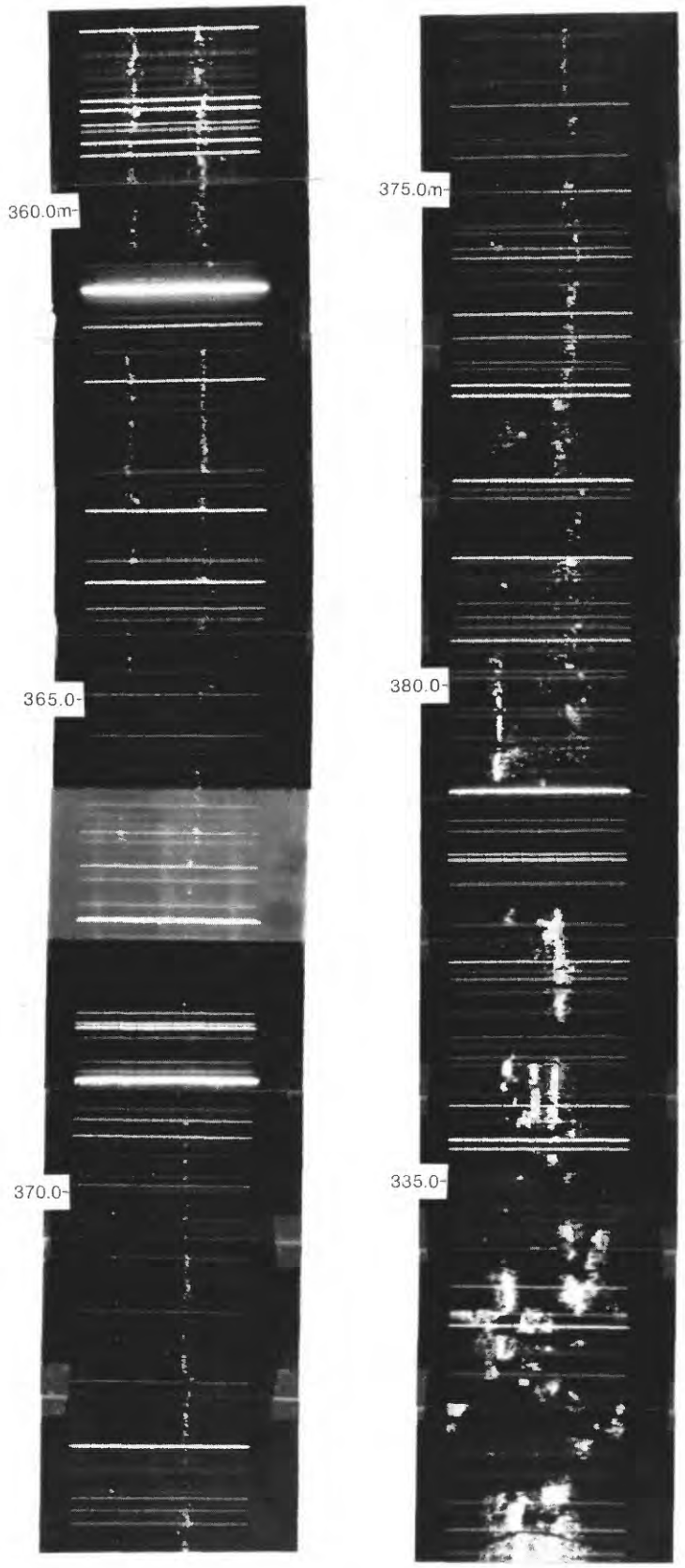
360.0m
365.0
370.0
375.0m
380.0
335.0

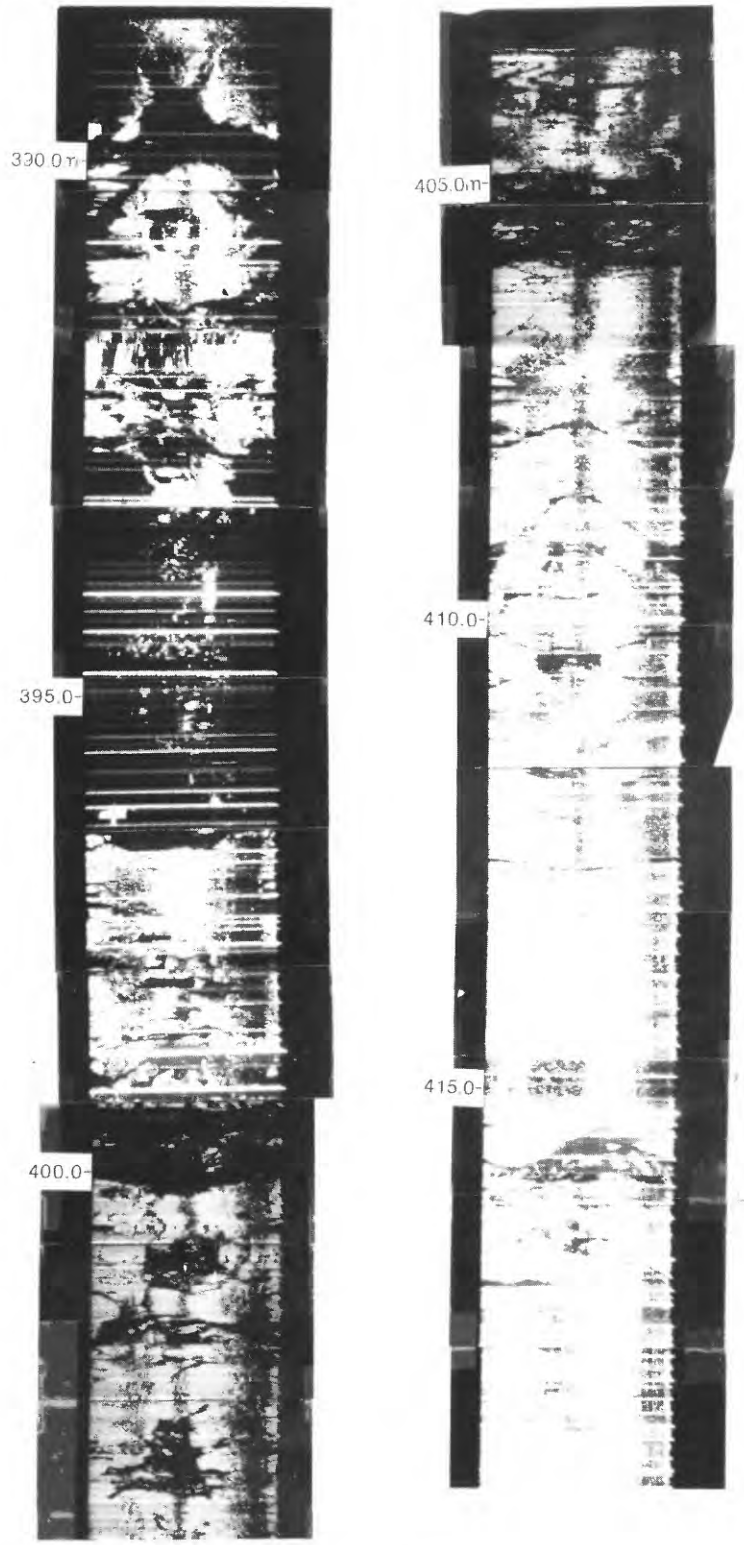
390.0m
395.0
400.0
405.0m
410.0
415.0

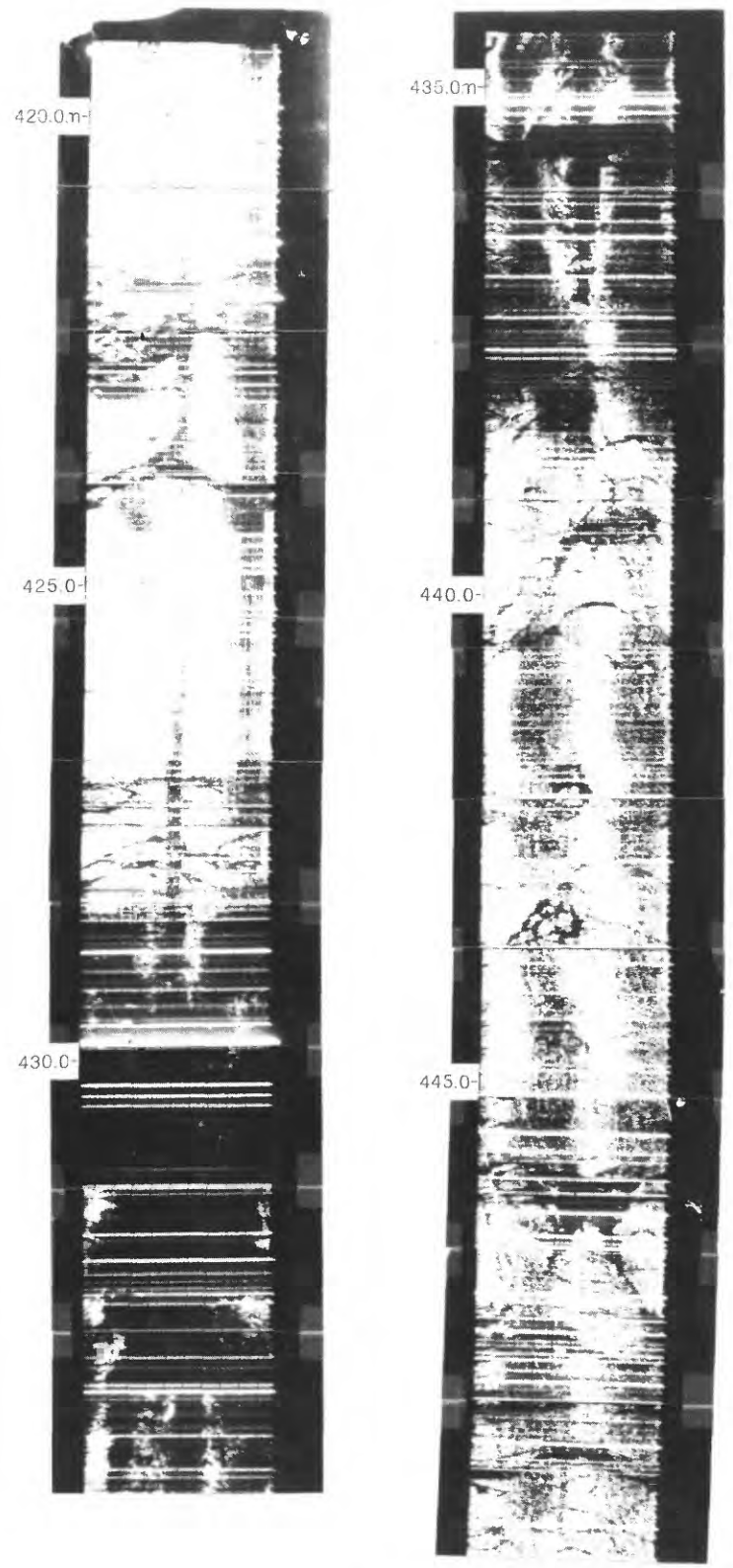
420.0m
425.0
430.0
435.0m
440.0
445.0

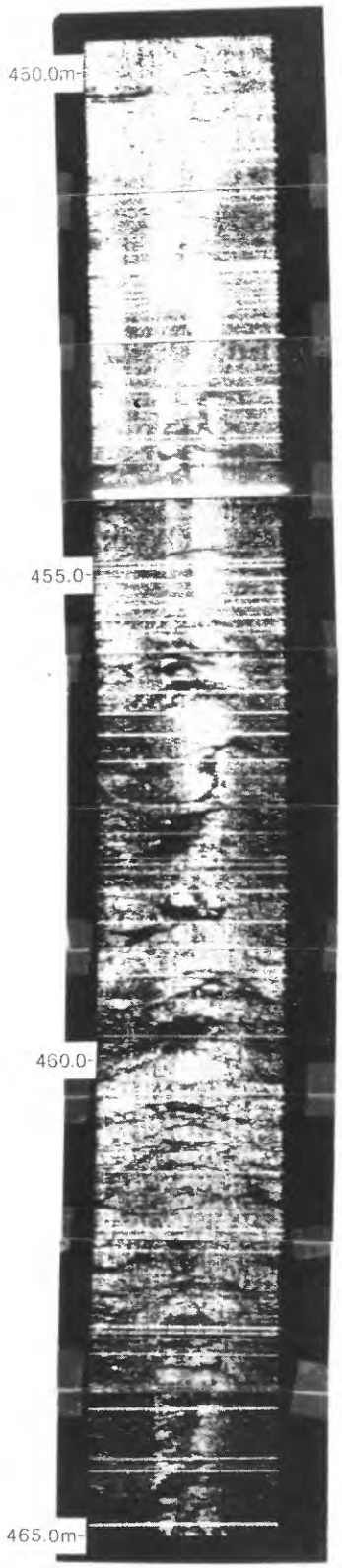
450.0m
455.0
460.0
465.0m